ceramics

MDPI

Article

Elastic Properties of Illite-Based Ceramics at Low Temperatures of Firing

Štefan Csáki [1,2,*], Tomáš Húlan [1], Anton Trník [1] and Igor Štubňa [1]

[1] Department of Physics, Constantine the Philosopher University in Nitra, Tr. A. Hlinku 1, 949 74 Nitra, Slovakia; atrnik@ukf.sk (A.T.)
[2] Department of Horticultural Machinery, Mendel University in Brno, Valticka 337, 691 44 Lednice, Czech Republic
* Correspondence: scsaki@ukf.sk

Abstract

Samples made from illitic clay were investigated using thermogravimetry (TG), thermodilatometry (TD) and dynamic mechanical analysis (DMA) during heating from room temperature to 300 °C. TG revealed three steps of mass loss: (a) the release of weakly bound H_2O (with the maximum rate at ~120 °C) from the pores, (b) a small mass loss event around 215 °C, (c) a small mass loss event near ~300 °C related to dehydration when H_2O molecules located in K-free sites of the illite interlayers are removed. TD indicated very small dimension changes for 20 °C → 300 °C. This behavior may result from two competing mechanisms, where the first one is regular thermal expansion and the second one is particle rearrangement caused by the removal of physically bound water. Young's modulus initially decreases during heating up to approximately 70 °C. Young's modulus subsequently increases exponentially, which may be explained by mechanisms analogous to those observed in the TD measurements. The activation energies derived from the exponential dependence $E(t)$ are 5.66 kJ/mol for the temperature interval 130–200 °C and 10.96 kJ/mol for the 200–280 °C range.

Keywords: illite; activation energy; Young's modulus

1. Introduction

Traditional clay bricks are made through an energy-intensive firing process. Currently, the traditional technology based on sintering of clays is still used, and incremental technological improvements remain the primary approach. The production of building ceramics is mostly based on illite- and kaolin-based clays. The illitic clays contain 40–80 mass% of illite. Quartz and feldspar are always present in naturally occurring clays, but montmorillonite, chlorite, micas, organic materials and small amounts of other minerals can also be present [1–3]. The mixture of clay and water is formed into a plastic ceramic body, which is subsequently dried and fired. During firing, the raw plastic ceramic mixture undergoes several physical and phase changes. Dehydroxylation, quartz transition, sintering, vitrification and high-temperature reactions are often studied—see, e.g., [2,4–11]—although dehydration and its influence on the physical properties of the fired ceramic body, which occurs at the lowest temperatures of firing, are rarely investigated.

The presence of water in the fired body microstructure has two causes—the remnants of the technological water used to prepare the plastic ceramic mixture and adsorbed moisture from surrounding air. This water is physically bound in the pores and surfaces of

Academic Editors: Gilbert Fantozzi and Vincent Garnier

Received: 21 April 2026
Revised: 22 May 2026
Accepted: 28 May 2026
Published: 29 May 2026

crystals, mainly on the basal and edge faces of the illite crystals. This is supported by the permanently negative surface charge which attracts polar water molecules. Some water molecules are located in the interlayer space of the illite structure but their amount is very low because this space is occupied by K^+ ions balancing the negative surface charge. The surface charge plays an important role in shrinkage when a sufficient amount of water escapes from the pores [12,13].

At the beginning of firing, when the temperature increases from room temperature up to ~300 °C, significant changes in material properties are observed. The Young's modulus of kaolin and illitic clay increases by 50–100% [7,14], sound velocity increases by 50% [15], mechanical strength increases by 83% [16] and DC electrical conductivity decreases by 6 orders of magnitude [17]. On the other hand, the volume changes are minimal [7,14]; the bulk density decreases only by ~4% [14]. The observed changes in physical properties are generally associated with the removal of physically bound water from pores and crystal surfaces.

The Young's modulus of the green clay-based material increases significantly at two stages during heating: from 20 °C to ~300 °C and from ~750 °C to the peak firing temperature (1000–1150 °C). Young's modulus increases 2.4 times within the 20–300 °C interval, compared to a 6.5-fold increase within the 750–1100 °C interval [18]. While the sintering stage has been extensively studied, the dehydration stage has received far less attention. To the best of our knowledge, the evolution of the Young's modulus of illite-based clays during the low-temperature dehydration stage (<300 °C) has not yet been systematically investigated. Because Young's modulus is essential for determining the optimal firing rate, its value must be measured at the actual temperature. Since low temperatures are critical for crack formation, Young's modulus represents an important parameter for estimating suitable firing conditions [19].

The evolution of Young's modulus in illite-based ceramics below 300 °C deserves detailed investigation because important physical and chemical transformations occurring in this temperature range strongly affect the material's elastic behavior and its susceptibility to crack formation. Processes such as the removal of physically bound water, dehydration of clay minerals, and initial structural rearrangements modify the stiffness of the ceramic body and generate internal stresses that may lead to damage during firing. Since Young's modulus is a key parameter for evaluating stress development and determining appropriate heating rates, accurate knowledge of its temperature dependence is essential for optimizing firing conditions and improving the quality of ceramic products.

The aim of this paper is to contribute to the experimental investigation of the elastic behavior of illite-based clay ceramics in the temperature range of 20–350 °C, with particular emphasis on the evolution of Young's modulus during the early stages of firing.

2. Materials and Methods

Samples prepared from illitic clay (Füzérradvány, Hungary) were investigated using thermogravimetry (TG), derivative TG (DTG), thermodilatometry (TD) and dynamic mechanical analysis (DMA) during heating. The chemical composition of the clay is shown in Table 1. The clay contains 67 mass % of illite, 1 mass % of montmorillonite, and 32 mass % of quartz.

Table 1. The chemical composition of illite (in mass%) [20].

SiO_2	Al_2O_3	Fe_2O_3	SO_3	CaO	MgO	K_2O	Na_2O	L.O.I.
55.69	29.18	0.87	0.10	0.31	1.36	7.74	0.01	4.74

The raw clay was first crushed and sieved to obtain a powder with particles not larger than 0.1 mm. Then 750 g of the powder were mixed with 250 g of distilled water to obtain a plastic mass from which cylindrical samples with diameter ∅11 mm were extruded. To reduce the temperature shift between TG, TD and DMA curves, the samples for these analyses were extruded with dimensions ∅11 × 30 mm for TD, ∅11 × 20 mm for TG/DTG and ∅11 × 120 mm for DMA. After open-air free drying, the samples contained ~3 mass% of physically bound water. A heating rate of 5 °C·min^{-1} was used for all thermal analyses.

A DMA analyzer [21] was used for the measurement of the resonant frequency of the sample at the actual temperature t during heating from 20 °C to 350 °C. The resonant frequency $f(t)$, the length $l(t)$, diameter $d(t)$, and mass $m(t)$ of the sample were used to calculate Young's modulus $E(t)$ according to [22]. Since the ratio length/diameter = 12 < 20, the value of Young's modulus must be multiplied by a correction coefficient T_{1c} = 1.091015 calculated for a circular cross-section and Poisson's ratio μ = 0.2. Young's modulus at temperature t is

$$E(t) = 1.6774 \frac{m_0 l_0^3}{d_0^4} \frac{\left[1 + \frac{\Delta m(t)}{m_0}\right]}{\left[1 + \frac{\Delta l(t)}{l_0}\right]} f^2(t) \quad (1)$$

where $\Delta l(t)/l_0$, $\Delta m(t)/m_0$, are relative linear thermal expansion and relative mass change of the sample. In deriving Equation (1), equal relative expansion of the sample in both the axial and radial directions was assumed. The values l_0 = 120 mm, d_0 = 11 mm, m_0 = 21.4 g are the initial length, diameter, and mass of the sample at room temperature, respectively.

As follows from Equation (1), the determination of $E(t)$ requires measuring the actual dimensions and mass of the sample during heating. This task was performed by TD and TG analyses. Given the relative expansion $\Delta l(t)/l_0$, as measured by the horizontal push-rod alumina dilatometer (Netzsch DIL 402C, Selb, Germany) on samples with dimensions ∅11 × 30 mm, the true length $l(t)$ and diameter $d(t)$ of the sample were calculated. Similarly, the true mass $m(t)$ was determined from the relative mass change $\Delta m(t)/m_0$ measured with TG/DTA analyzer Derivatograph 1000 (MOM Budapest, Budapest, Hungary) [23] on cylindrical samples with dimensions of 11 × 20 mm^2. All thermal analyses were performed in a static air atmosphere. Three independent measurements were carried out for each experiment to verify the repeatability and reliability of the obtained results.

The bulk density ρ and total porosity P were estimated from a volume V of the sample, its mass m and mineral composition. Since the crystal densities of the components are known, the volume V_0 of the poreless sample can be calculated. The bulk density determined from sample mass and volume is $\rho = \frac{m}{V}$ and porosity $P = 1 - (V_0/V)$. It should be noted that the presented values of bulk density and porosity represent estimations derived from dimensional and compositional data rather than direct experimental measurements.

3. Results and Discussion

The results of TG and DTG of the illitic clay (Figure 1) exhibit three steps of mass loss. These steps reflect three overlapping processes. The first step corresponds to the release of weakly bound H_2O (between 20 °C and 300 °C with the maximum loss rate at ~120 °C) from the pores. The interval is rather large, which indicates differences in attractive forces between water molecules and crystal surfaces. A small shoulder is visible on the DTG peak of the main dehydration at ~210 °C indicating a hidden DTG peak which represents a small amount of the escaping water vapor. The origin of this second stage of mass loss remains unclear. Since its temperature interval is relatively narrow, specific charged defects may interact more strongly with water molecules, so higher energy is necessary to remove them. As noted above, DC conductivity decreases by 6 orders of magnitude between 70 °C and 170 °C. This behavior is likely associated with the decrease

in the concentration of H^+ and OH^- ions generated by the ionization of water. These ions, after recombination, as water molecules simultaneously evaporate with other water molecules from the sample. The results of DC conductivity are consistent with TG and DTG results and point out the importance of electrostatic forces within the clay microstructure at low temperatures. The third step, in accordance with [24], is characterized by a DTG minimum at ~300 °C. It is attributed to the release of H_2O molecules located in K^+-free sites within the illite interlayers.

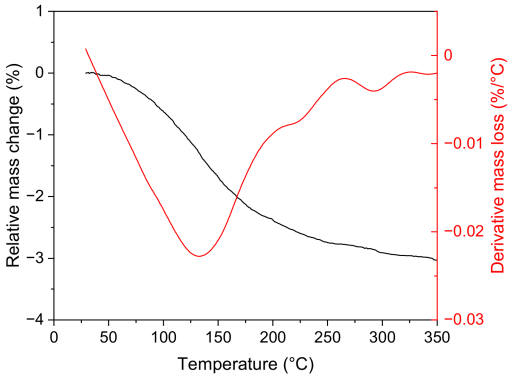

Figure 1. TG and DTG of the illitic clay.

The TD curve of illitic clay is shown in Figure 2. At low temperatures, very small dimension changes are measured. This behavior may be attributed to two competing mechanisms, where the first one is regular (linear) thermal expansion and the second one is reduction in d_{001} basal spacing due the gradual loss of interlayer water [25–27]. The microstructure of the green sample is full of small pores and capillaries, and water vapor is inside them. According to [28], internal steam pressure of several MPa must be generated to surpass the surface stress which happens at higher drying temperature. As the drying temperature increases, the drying process is accelerated and the drying shrinkage of the fired sample decreases. The gaps among the crystals decrease, while the grains themselves expand [26,27]. At the same time due to the great number of pores and capillaries and their increased size resulted from more intensive drying, the total shrinkage decreases. The drying temperature and the drying dynamics can essentially influence the microstructure and physical properties of the brick at the lowest firing temperatures.

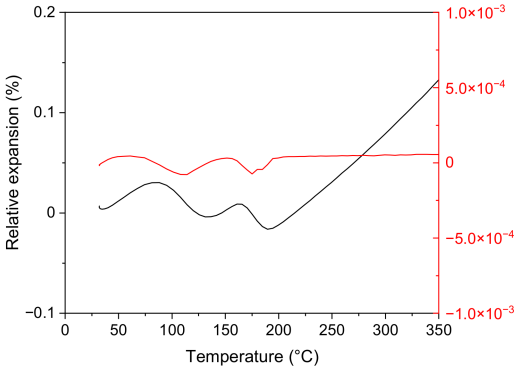

Figure 2. TD and coefficient of linear thermal expansion (CLTE) of the illitic clay.

A development of Young's modulus (E) within the low-temperature region is illustrated in Figure 3. Young's modulus begins to decrease immediately upon the onset of heating. This transient phenomenon persisting up to ~70 °C is regularly observed when DMA of air-dried kaolin-based and illite-based clays is performed [29]. The origin of this decrease remains to be fully elucidated.

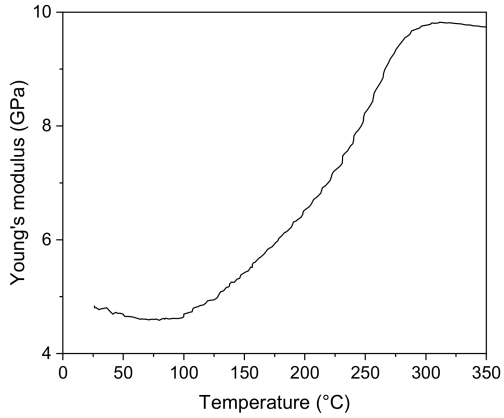

Figure 3. Young's modulus of the illitic clay.

Following this temporary decrease, Young's modulus begins to increase. This enhancement may be associated with the release of water from pores, which allows a reduction in inter-crystalline distances. The formation of stronger inter-crystalline contacts may contribute to the observed exponential increase in Young's modulus (Figure 4). When the dependence $E(t)$ is presented in Arrhenius coordinates, the experimental data are separated into two linear segments with a transition point ~200 °C. The activation energies (E_a) derived from these segments are 5.66 kJ/mol for the temperature interval 130–200 °C and 10.96 kJ/mol for the 200–280 °C range (Figure 4). Calculation of E_a was performed by multiplying the slope of the linear curve (Table 2) with a constant of 19.147 (obtained as multiplication of the universal gas constant R with 2.303 due to the use of $\log_{10}$ instead of ln). These energies may correspond to thermally activated microstructural changes. The transient temperature of 200 °C is the same as that around which the hidden DTG peak in Figure 1 arose. Similar behavior has also been observed in illitic clays of various provenances and compositions. The obtained results suggest that microstructural changes may occur (expansion of crystal volume, decrease in interparticle distances [26,27]) as a consequence of simultaneous heating and dehydration.

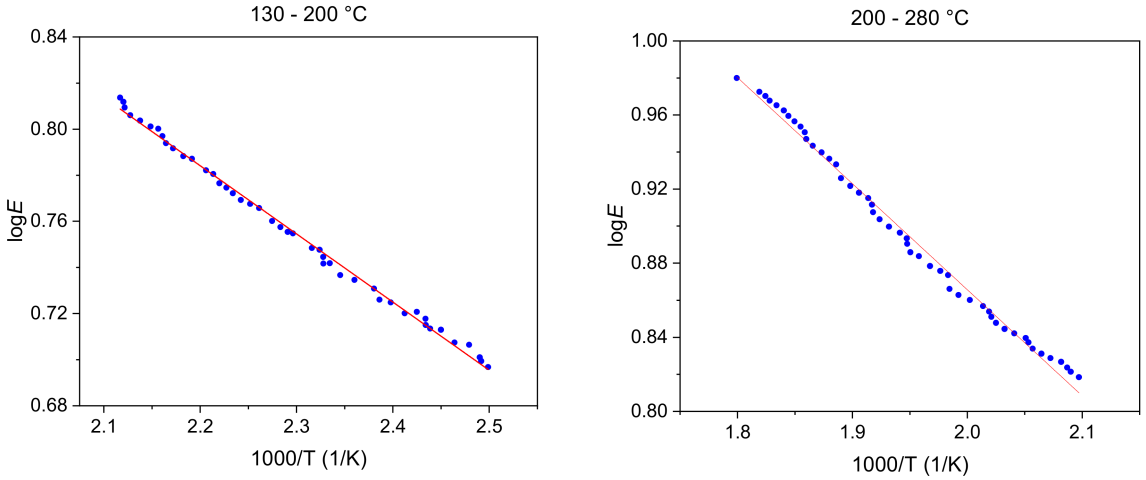

Figure 4. Exponential increase in Young's modulus (E) between 130 °C and 280 °C (red line—fitted curve).

Simultaneously, a common thermal expansion takes place. This process leads to bond elongation within the illite crystals (and other), which also causes their weakening, and consequently, reduces Young's modulus. Similar behavior has been reported for various metals and ceramics. Since the increase in Young's modulus during heating

was experimentally observed, the effect of the thermal expansion on Young's modulus is evidently weaker than the competing mechanism of crystal compaction. In the dry form, the illite plate-like crystals are held together by van der Waals forces. The escape of water from the pores and the resulting direct contact between the crystals may allow van der Waals interactions to act more effectively.

Table 2. Parameters of the fitted linear curve.

	130–200 °C	**200–280 °C**
Intercept	1.435	2.011
Slope	−0.296	−0.573
R-square	0.996	0.992
E_a (kJ/mol)	5.66	10.96

Young's modulus is proportional to the bulk density. Since the sample dimensions change very slowly (~0.15% between 20 °C and 250 °C) and the mass loss changes faster (~3% between 20 °C and 250 °C), the bulk density slightly decreases ρ(250 °C) = 0.95ρ(20 °C). The improvement of the contacts among crystals overcomes the slight decrease in bulk density and the minor increase in porosity, which changes from P(20 °C) = 37% to P(250 °C) = 38.5%. When the water molecules escaped, thermal expansion remains the only mechanism affecting Young's modulus. It shows a slight decrease above 300 °C [14,29]. The change in the microstructure during drying proposed in [28] can explain a small increase in porosity and very slight increase in the sample volume, but not the increase in Young's modulus. The thermal expansion and porosity generally reduce Young's modulus. This requires another mechanism which increases Young's modulus. A possible explanation is the tighter packing of crystals above 70 °C and the expansion of pores due to water vapor escape at the lowest temperatures (20 °C → 70 °C) can explain a small decrease in Young's modulus. The significant increase in Young's modulus (from E(70 °C) = 5 GPa to E(300 °C) = 10 GPa) may therefore be associated with progressive improvement of inter-crystalline contacts during dehydration.

4. Conclusions

Illitic clay samples were investigated by thermogravimetric (TG), thermodilatometric (TD), and dynamic mechanical analyses (DMA) during heating from room temperature to 300 °C in order to evaluate the influence of dehydration on their thermal and elastic behavior. The obtained results demonstrated that the dominant process within the investigated temperature range was the gradual removal of physically bound water. A pronounced release of pore water was observed with a maximum rate at approximately 120 °C, accompanied by a minor mass-loss event near 215 °C and a further small mass decrease around 300 °C, which may be related to the release of H_2O molecules from K^+-free interlayer sites in illite.

Despite the ongoing dehydration processes, only very small dimensional changes were detected during heating. This behavior may be explained by the competition between conventional thermal expansion and reduction in distances between the individual crystals associated with water removal from pores and crystal surfaces.

Young's modulus initially decreased between room temperature and approximately 70 °C, after which it increased exponentially from approximately 5 GPa at 70 °C to 10 GPa at 300 °C. This increase in Young's modulus may be associated with progressive improvement of inter-crystalline contacts resulting from dehydration-induced microstructural changes. The Arrhenius representation of the experimental data revealed two distinct temperature intervals characterized by activation energies of 5.66 kJ/mol (130–200 °C) and 10.96 kJ/mol

(200–280 °C), suggesting the presence of two thermally activated processes occurring during dehydration.

The presented results contribute to a better understanding of the elastic behavior of illite-based clays during the early stages of firing. Since low-temperature dehydration processes may significantly influence stress evolution and crack formation, the obtained findings may be useful for optimizing firing schedules and improving the quality of ceramic products.

Author Contributions: Conceptualization, I.Š.; methodology, T.H.; validation, Š.C. and I.Š.; formal analysis, Š.C.; investigation, T.H. and Š.C.; data curation, A.T.; writing—original draft preparation, I.Š. and A.T.; writing—review and editing, A.T. and Š.C.; funding acquisition A.T. and Š.C. All authors have read and agreed to the published version of the manuscript.

Funding: This research was funded by the Czech Science Foundation, grant number 24-12226S.

Data Availability Statement: The datasets generated during and/or analyzed during the current study are available from the corresponding author on reasonable request.

Conflicts of Interest: The authors declare no conflicts of interest.

References

1. Gömze, L.A.; Gömze, L.N.; Kurovics, E.; Benedek, G. Conventional Brick Clays as a Challenge of Materials Science—New Explanation of Drying Sensitivities. *IOP Conf. Ser. Mater. Sci. Eng.* **2019**, *613*, 012005. [CrossRef]
2. Ferrari, S.; Gualtieri, A.F. The Use of Illitic Clays in the Production of Stoneware Tile Ceramics. *Appl. Clay Sci.* **2006**, *32*, 73–81. [CrossRef]
3. Sedmale, G.; Korovkins, A.; Seglins, V.; Lindina, L. Application of Chemical Trated Illite Clay for Development of Ceramics Products. *IOP Conf. Ser. Mater. Sci. Eng.* **2013**, *47*, 012056. [CrossRef]
4. Gualtieri, A.F.; Ferrari, S.; Leoni, M.; Grathoff, G.; Hugo, R.; Shatnawi, M.; Paglia, G.; Billinge, S. Structural Characterization of the Clay Mineral Illite-1M. *J. Appl. Crystallogr.* **2008**, *41*, 402–415. [CrossRef]
5. Aras, A. The Change of Phase Composition in Kaolinite- and Illite-Rich Clay-Based Ceramic Bodies. *Appl. Clay Sci.* **2004**, *24*, 257–269. [CrossRef]
6. Hanykýř, V.; Kutzendörfer, J. *Technology of Ceramics*; Silikátový svaz: Praha, Czech Republic, 2008.
7. Knapek, M.; Húlan, T.; Minárik, P.; Dobroň, P.; Stubňa, I.; Stráská, J.; Chmelík, F. Study of Microcracking in Illite-Based Ceramics during Firing. *J. Eur. Ceram. Soc.* **2016**, *36*, 221–226. [CrossRef]
8. Escalera, E.; Antti, M.L.; Odén, M. Thermal Treatment and Phase Formation in Kaolinite and Illite Based Clays from Tropical Regions of Bolivia. *IOP Conf. Ser. Mater. Sci. Eng.* **2012**, *31*, 012017. [CrossRef]
9. Norton, F.H. *Fine Ceramics Technology and Applications*; McGraw-Hill: New York, NY, USA, 1970.
10. Číčel, B.; Novák, I.; Horváth, I. *Mineralogy and Crystallochemistry of Clays*; VEDA: Bratislava, Slovakia, 1981.
11. Drits, V.A.; McCarty, D.K.; Derkowski, A. Mixed-Layered Structure Formation during Trans-Vacant Al-Rich Illite Partial Dehydroxylation. *Am. Mineral.* **2012**, *97*, 1922–1938. [CrossRef]
12. Kumari, N.; Mohan, C. Basics of Clay Minerals and Their Characteristic Properties. In *Clay and Clay Minerals*; Morari Do Nascimento, G., Ed.; IntechOpen: Rijeka, Croatia, 2021.
13. Tournassat, C.; Bourg, I.C.; Steefel, C.I.; Bergaya, F. Surface Properties of Clay Minerals. In *Developments in Clay Science*; Elsevier: Amsterdam, The Netherlands, 2015; Volume 6, pp. 5–31.
14. Štubňa, I.; Húlan, T.; Kaljuvee, T.; Vozár, L. Investigation of Dynamic Mechanical Properties of Estonian Clay Arumetsa during Firing. *Appl. Clay Sci.* **2018**, *153*, 23–28. [CrossRef]
15. Trník, A.; Štubňa, I.; Moravčíková, J. Sound Velocity of Kaolin in the Temperature Range from 20 °C to 1100 °C. *Int. J. Thermophys.* **2009**, *30*, 1323–1328. [CrossRef]
16. Štubňa, I.; Šín, P.; Trník, A.; Veinthal, R. Mechanical Properties of Kaolin during Heating. *Key Eng. Mater.* **2012**, *527*, 14–19. [CrossRef]
17. Podoba, R.; Štubňa, I.; Trnovcová, V.; Trník, A. Temperature Dependence of DC Electrical Conductivity of Kaolin. *J. Therm. Anal. Calorim.* **2014**, *118*, 597–601. [CrossRef]
18. Húlan, T.; Štubňa, I.; Shishkin, A.; Ozolins, J.; Csáki, S.; Bačík, P.; Fridrichová, J. Development of Young's Modulus of Natural Illitic Clay during the Heating and Cooling Stages of Firing. *Clay Miner.* **2019**, *54*, 229–233. [CrossRef]
19. Gregorová, E.; Pabst, W.; Nečina, V.; Uhlířová, T.; Diblíková, P. Young's Modulus Evolution during Heating, Re-Sintering and Cooling of Partially Sintered Alumina Ceramics. *J. Eur. Ceram. Soc.* **2019**, *39*, 1893–1899. [CrossRef]

20. Csáki, Š.; Kovács, T.; Keppert, M.; Pommer, V.; Lukáč, F.; Knapek, M.; Minárik, P.; Trník, A. Development of Young's Modulus of Illite/Smectite—$CaCO_3$ Composites After Various Firing Temperatures. *Crystals* **2025**, *15*, 592. [CrossRef]
21. Húlan, T.; Štubňa, I.; Al-Shantir, O.; Trník, A. The Apparatus for Thermomechanical Analysis of Clay-Based Ceramics. *Meas. Sci. Rev.* **2023**, *23*, 130–135. [CrossRef]
22. *ASTM E 1876-09*; Standard Test Method for Dynamic Young's Modulus, Shear Modulus and Poisson's Ratio by Impulse Excitation of Vibration. ASTM International: Philadelphia, PA, USA, 2009.
23. Podoba, R.; Trník, A.; Podobník, Ľ. Upgrading of TGA/DTA Analyzer Derivatograph. *Építőanyag* **2012**, *64*, 28–29. [CrossRef]
24. Drits, V.A.; McCarty, D.K. The Nature of Structure-Bonded H_2O in Illite and Leucophyllite from Dehydration and Dehydroxylation Experiments. *Clays Clay Miner.* **2007**, *55*, 45–58. [CrossRef]
25. Jia, J.; Wu, D.; Lin, J.; Jiang, X. Molecular Dynamics Simulation of Illite: From Particle Associations to Hydration Properties. *Appl. Clay Sci.* **2023**, *234*, 106850. [CrossRef]
26. Wang, G.; Wang, H.; Zhang, N. In Situ High Temperature X-Ray Diffraction Study of Illite. *Appl. Clay Sci.* **2017**, *146*, 254–263. [CrossRef]
27. Clanton, U.S. High-Temperature X-Ray Diffraction. Master's Thesis, The University of Texas, Austin, TX, USA, 1960.
28. Gömze, L.A.; Gömze, L.N. Relations between the Material Structures and Drying Properties of Ceramic Bricks and Roof Tiles. *Epa.-JSBCM* **2008**, *60*, 102–107. [CrossRef]
29. Húlan, T.; Kaljuvee, T.; Štubňa, I.; Trník, A. Investigation of Elastic and Inelastic Properties of Estonian Clay from a Locality in Kunda during Thermal Treatment. *J. Therm. Anal. Calorim.* **2016**, *124*, 1153–1159. [CrossRef]